Regular Article

ANALYTICAL AND BIOANALYTICAL CHEMISTRY RESEARCH

Published by the Iranian Chemical Society

Anal. Bioanal. Chem. Res., Vol. 9, No. 1, 113-121, January 2022.

A Sensitive Electrochemical Sensor Due to Novel Bionanocomposite to Determine Tartrazine

Reza Zarrin and Reza Emamali Sabzi*

Department of Analytical Chemistry, Faculty of Chemistry, Urmia University, Urmia, Iran

(Received 4 March 2021 Accepted 21 September 2021)

A novel composite was fabricated utilizing gold nanoparticle-modified (AuNPs) reduced graphene oxide (rGO) composite and acetone-extracted propolis (AEP) for electrochemical sensors on screen-printed electrodes (AuNPs/rGO/AEP/SPE) using electrochemical approaches for tartrazine (Tz) detection. Electrochemical experiments and scanning electron microscopy (SEM) were applied for electrode characterization. The diagrams of provided cyclic voltammetry (CV) indicated that the highest Tz oxidation catalytic activity was provided for AuNPs/rGO/AEP/SPE followed by rGO/AEP/SPE, GO/AEP/SPE, and SPE. Utilizing differential pulse voltammetry (DPV) techniques in the range of 0.004 to 2 µM with a detection limit of 3 nM, the range for Linear Tz calibration curves were provided at AuNPs/rGO/AEP/SPE. The findings of this study showed that AuNPs/rGO/AEP/SPE could be applied for Tz detection with high stability, low detection limit, and high sensitivity, which appear to be helpful in the manufacture of portable sensors for use in the food industry.

Keywords: Screen-printed electrodes, Tartrazine, Differential pulse voltammetry, Electrochemical detection

INTRODUCTION

To produce various foods and drinks, the food dye Tz ($C1_6H_9N_4Na_3O_9S_2$) is generally considered as an additive. However, Tz can elicit asthmatic and allergic responses in persons consuming particular drugs like benzoic acid and aspirin, particularly those with weakened immune systems [1]. High Tz concentrations can lead to cancer, neurobehavioral issues, reproductive toxicity, and childhood hyperactivity disease [2]. The maximum allowable concentration of Tz dye in non-alcoholic drinks containing added flavors and/or juices is 100 µg ml^{-1} (in combined or segregated modes) [3]. Therefore, surveying Tz in food products is quite important. Different techniques for evaluating Tz have been established, such as fluorescence emission spectrometry [4], visible spectrophotometry [5], high-performance liquid chromatography (HPLC) [6], and tandem mass detector HPLC (HPLC-MS/MS) [7]. The benefits of this composite are its convenience, high flexibility, good sensitivity, and low cost [8]. To evaluate Tz, the development of electrochemical techniques has been advanced.

Graphene has become quite popular because of its excellent conductivity, greatly surface area, significant amount of edge-plan-like defects, and high catalytic activity [9], making it applicable in multiple utilizations such as supercapacitors [10], fuel cells, sensor materials, and composites [11]. Multiple sensors like exfoliated graphite-glassy carbon electrode (EG-GCE) [12], fluorescein/rGO complex dye sensor [13], and AuNPs- modified GCE [14] use grapheme to identify Tz electrochemically. Furthermore, AuNPs have presented excellent electrical conductivity, biocompatibility, good adsorption capacity, and high catalytic activity [15]. Thus, integrating the benefits of Au and graphene by fabricating AuNPs/rGO composites as sensors has high importance. In practice, sensors like AuNPs/rGO/Chit [12], rGO/AuNPs/SPE [16], and rGO/AuNPs/GCE [17] are applied for detecting β-

Corresponding author. E-mail: r.emamalisabzi@urmia.ac.ir

nicotinamide adenine dinucleotides as well as herbicide diuron and mercury(II) isomers. Therefore, utilizing AuNPs/rGO composite materials for detecting Tz with electrochemical methods has rarely been investigated.

Propolis (bee glue) resin is applied by bees in beehives [18] and is popular for use in a large variety of cosmetics and medicines because of its anti-tumor, antioxidant, and antimicrobial properties [19-21]. The most growing extract of ethanol from propolis, among other solvents, is the most common [22]. By applying multiple analytical approaches, it was determined that propolis consists of 45% resin, 35% wax, and 20% inert materials [23]. Organic solvents are applied to classify constituents, especially wax, as they are insoluble in polar solvents, such as water [24]. Propolis has extraordinary mixed features, like good biocompatibility, high mechanical strength, non-toxicity, good adhesion, excellent membrane-forming capacity against water, and sensitivity to chemical modification due to different reactive functional groups [25-27].

Acetone-extracted propolis (AEP) was used for the first time, and a simple route was suggested for the synthesis of AuNPs-loaded functionalized rGO for the detection of Tz. The developed approach integrated the electrical conductivity of AuNPs and the tremendous particular surface area of graphene. Furthermore, it is a promising approach for practical utilization in environmental control and biological analysis.

EXPERIMENTAL

Reagents and Apparatus

Considering the Hummers and Offerman method, GO was fabricated from graphite. Graphite powder was purchased from Merck Company, Germany. Tz, potassium chloride (KCl), sodium borohydride ($NaBH_4$), potassium hydroxide (KOH), potassium ferricyanide/ferrocyanide ($K_4[Fe(CN)_6]/K_3[Fe(CN)_6]$) for impedance detection, and gold acid chloride trihydrate ($HAuCl_4 \cdot xH_2O$), all analytical grade, were provided by Sigma-Aldrich. Acetone dimethyl formamide and hexane were bought from Merck Company, Germany. A brown-colored propolis sample was gathered from honey bee colonies in Urmia City in northwestern Iran in the summer of 2019. Using a frequency response analyzer (FRA4.9), electrochemical experiments were guided on an Autolab PGSTAT30 Potentiostat/Galvanostat fitted and managed by the software, General Purpose Electrochemical System (GPES4.9) (Eco Chemie, Utrecht, Netherlands).

Pretreatment of Screen Printed Electrodes (SPE)

To improve the voltammetric behaviors of SPE, electrochemical preconditioning is a facile and efficient method. Electrodes were triggered in 100 µl PBS solution utilizing an anodic potential (in the range of +0.2 V to +2 V) for 5 min. Then, electrodes were washed with distilled water after activation, which provided for modification.

Preparing AuNPs/rGO/AEP Nanocomposite Modified SPE

AuNPs/rGO/AEP was suggested as follows: First, propolis was dissolved in 10 ml acetone under stirring for one hour at room temperature. While waiting for the wax to dissolve completely, AEP solution (2 wt%) was provided. Then, the mixture was centrifuged at 3000 rpm, and the yellow supernatant solution was gathered for future stages and stored while unutilized in the refrigerator at 4 °C. GO was synthesized using the approach reported by Hummers [28]. GO (10 mg) was dispersed in 10 ml deionized water to prepare GO nanosheets. The provided solution was sonicated in an ice-water bath (0 °C) for one hour. GO aqueous solution 10^{-3} g l^{-1} was constantly stirred at 180 °C for two hours. The formation of rGO was indicated by changes in the solution color from yellow-brown to black. 50 ml $HAuCl_4$ (0.05%) was added drop-wise into the prepared liquid mixture and stirred for 20 min. Then, one ml sodium borohydride solution (1%) was added and the mixture was boiled for 1 h, then stirred until the mixture had cooled to room temperature. The cooled mixture was centrifuged for 20 min at 10000 rpm and washed with water. AuNPs/rGO/AEP films were provided to prepare a homogeneous dispersion of AuNPs/rGO by mixing 2% AEP solution and AuNPs/rGO powder and stirring for three hours. Then, 5 µl of the as-prepared mixture was added to a pretreated SPE, which was dried for three hours at room temperature in a vacuum desiccator, supplying a ready-to-use AuNPs/rGO/AEP/SPE.

RESULTS AND DISCUSSION

Cyclic Voltammetry (CV) of Hexacyanoferrate (HCF)

In the presence of 1 mM $Fe(CN)_6^{-3}/Fe(CN)_6^{-4}$ as a redox probe (0.1 M KCl), the cyclic voltammograms of different modified electrodes in the potential range of -0.2 to 0.4 V are shown in Fig. 1. Due to the figure curve, a reversible cyclic voltammogram for bare SPE was displayed by redox probe $Fe(CN)_6^{-3}/Fe(CN)_6^{-4}$. The cyclic voltammograms of bare SPE, GO/AEP/SPE, rGO/AEP/SPE, and AuNPs/rGO/AEP/SPE in 1 mmol $Fe(CN)_6^{-3}/Fe(CN)_6^{-4}$ solution were provided, as indicated in Fig. 1. A pair of reversible redox peaks was displayed in voltammograms. Therefore, redox peak intensities were increased in the following order: GO/SPE, bare SPE, rGO/AEP/SPE, and AuNPs/rGO/AEP/SPE. Due to the low electrical conductivity, GO serves as an insulating layer, which makes transferring charge interfacial more difficult. For this reason, the lowest current of redox peak was provided on GO/SPE [29]. By reducing GO to rGO, based on the reconstructed conductive carbon conjugate network and increasing the effective surface, the redox peak current was significantly increased [30]. By mixing rGO with AuNPs, the redox peak current was more increased, based on which, it was suggested that the electrochemical activity of the working electrode could be enhanced by both AuNPs and rGO sheets, and this composite could effectively increase the ability to transfer electrons.

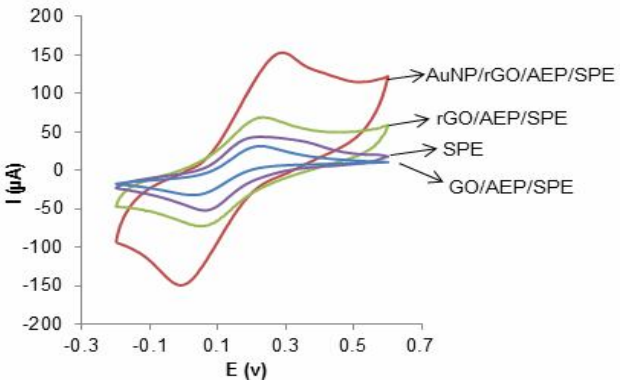

Fig. 1. Cyclic voltammograms of 1.0 mM $Fe(CN)_6^{3}/Fe(CN)_6^{-4}$ containing 0.1 M KCl recorded at SPE, GO/AEP/SPE, rGO/AEP/SPE, and AuNPs/rGO/AEP/SPE.

Scanning Electron Microscopy Analysis of AuNPs/rGO/AEP Nanocomposite

Scanning electron microscopy (SEM) was used to survey the nature of AuNPs/rGO/AEP nanocomposite. SEM images of SPE, rGO/AEP/SPE, and AuNPs/rGO/AEP/SPE are given in Figs. 2A, B, and C, respectively. Before spotting, SPE presented smooth surfaces with some wrinkles (Fig. 2A). After spotting, rough surfaces were witnessed due to the formation of rGO/AEP/SPE and AuNPs/rGO/AEP/SPE on electrode surfaces (Fig. 2C). Two materials had such distinct morphologies. The surfaces of

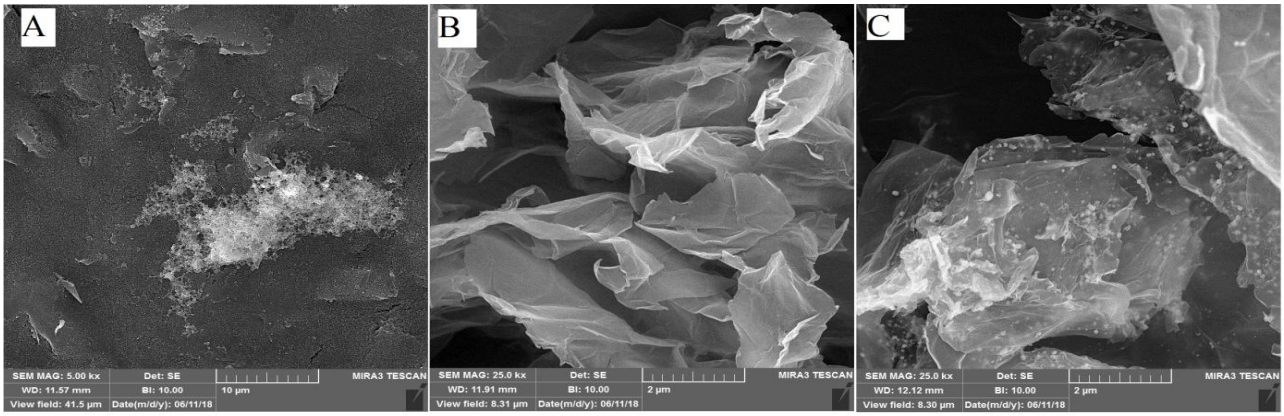

Fig. 2. SEM images of bare SPE (A), rGO/AEP/SPE (B) and AuNPs/rGO/AEP/SPE (C).

rGO/AEP/SPE and AuNPs/rGO/AEP/SPE nanocomposites were relatively rough with distinct interstices that were suitable for enhancing activity sites and analyte accumulation.

Electrochemical Characterization the Interface of Different Modified Electrodes

The electrochemical impedance spectroscopy (EIS) can be used to test conductivity of different electrode by utilizing and multiple modification steps, chemical transition and processes associated with the conductive electrode [31]. Figure 3 presents the EIS diagrams of different modified electrodes. In the EIS, the portion of the semi-circle section at higher frequencies corresponds to the electron transfer-limited process. Applying an electrochemical probe (0.1 M KCl) of 1 mM $Fe(CN)_6^{-}/Fe(CN)_6^{-4}$, the diameter refers to electron transfer resistance (R_{et}). In this approach, resistance against charge transfer can be measured by applying the semicircle diameter; as it is increased, resistance against charge transfer is also increased. Figure 3 indicates the behaviors of different modified electrodes at EIS. GO/SPE presented a semicircle with a relatively large diameter (1050 Ω) which showed high R_{et}, compared to bare SPE (945 Ω). The R_{et} value of rGO/AEP/SPE (750 Ω) was significantly decreased due to the reduced conductivity of the GO sheets. The R_{et} value of AuNPs/rGO/AEP/SPE (552 Ω) compared to other constructed electrodes is highly reduced due to the simultaneous presence of decreased GO sheets and AuNPs on the electrode surface.

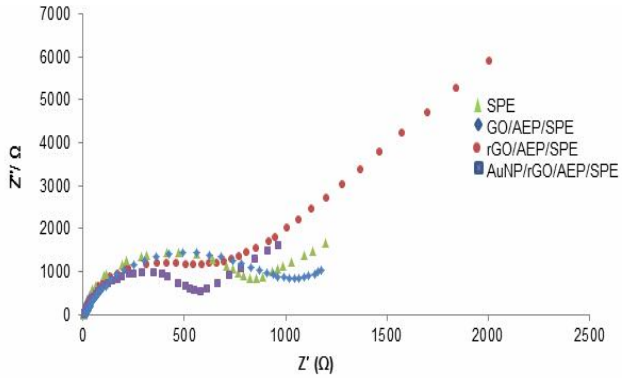

Fig. 3. Nyquist plots for 1.0 mM $Fe(CN)_6^{-3}/Fe(CN)_6^{-4}$ in 0.1 M KCl solution recorded at SPE, GO/AEP/SPE, rGO/AEP/SPE, and AuNPs/rGO/AEP/SPE.

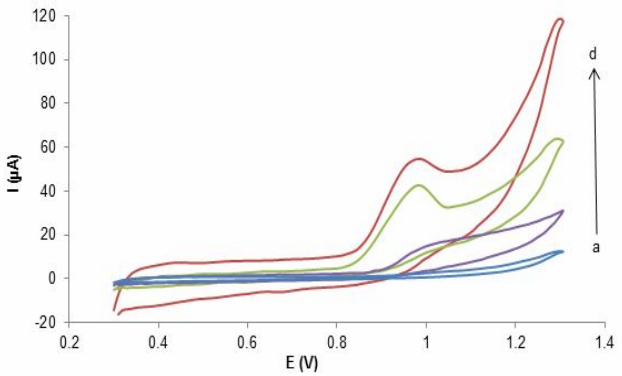

Fig. 4. Cyclic voltammetry of (a) SPE, (b) GO/AEP/SPE, (c) rGO/AEP/SPE and (d) AuNPs/rGO/AEP /SPE in the presence of 5 µM Tz, 0.1 M PBS (pH = 6), scan rate: 50 mV s^{-1}.

Electrochemical Behavior of Tz on Different Modified Electrodes

Using cyclic voltammetry CV, the electrocatalytic oxidation of Tz on bare and modified electrodes was investigated. Figure 4 illustrates the cyclic voltammograms of bare SPE (a), GO/AEP/SPE (b), rGO/AEP/SPE (c), and AuNPs/rGO/AEP/SPE (d) in PBS solution involving 5 µM Tz. On bare SPE, a small oxidation peak assigned to Tz oxidation appeared at 1.05 V. Tz oxidation currents on GO/SPE (b) were higher than that on SPE, which indicates the evident catalytic activity of GO toward Tz oxidation. GO sheets on the SPE surface had strong adsorptive capability toward Tz due to the formation of different interactions, such as electrostatic interaction, hydrophobic force, and hydrogen bonds. Appling GO immobilization on SPE surfaces, higher Tz oxidation currents were displayed (B) due to bare SPE (A), possibly because of the increased effective surface area of the modified electrode. Moreover, Tz peak currents showed a considerable enhancement on rGO/AEP/SPE (C) and AuNPs/rGO/AEP/SPE (D) compared to other modified SPEs. The higher electrocatalytic behavior of Au/rGO/AEP/SPE may primarily be due to the advent of graphene, which offers a large loading platform for AuNPs that could increase efficient electrode surface area and improve the transfer of electrons to the electrode [15,32].

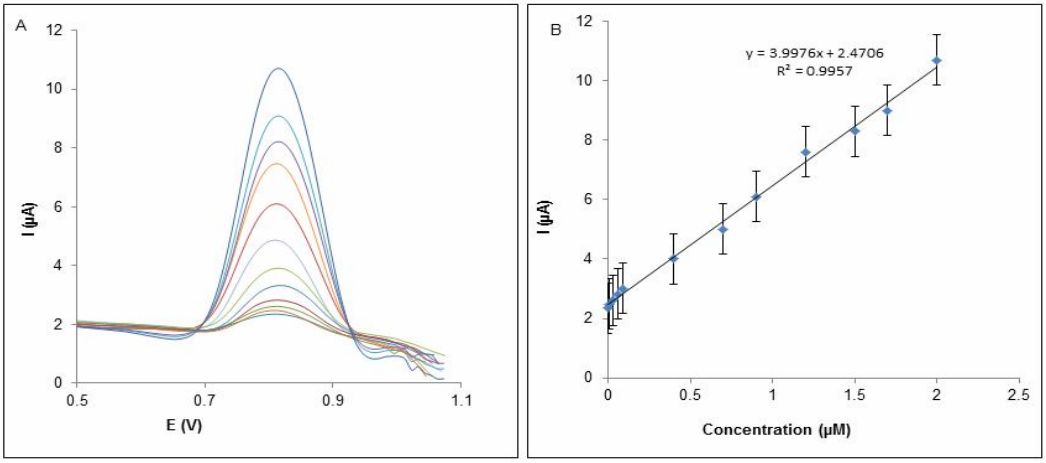

Fig. 5. (A) DPVs of AuNPs/rGO/AEP/SPE in 0.1 M PBS at (pH 6.0) after Tz addition to give final solution concentrations in the range of 0.004 µM to 2 µM, scan rate: 50 mV s^{-1}, and 2.0 min accumulation time; (B) calibration plot of the oxidation peak currents as a function of Tz concentrations.

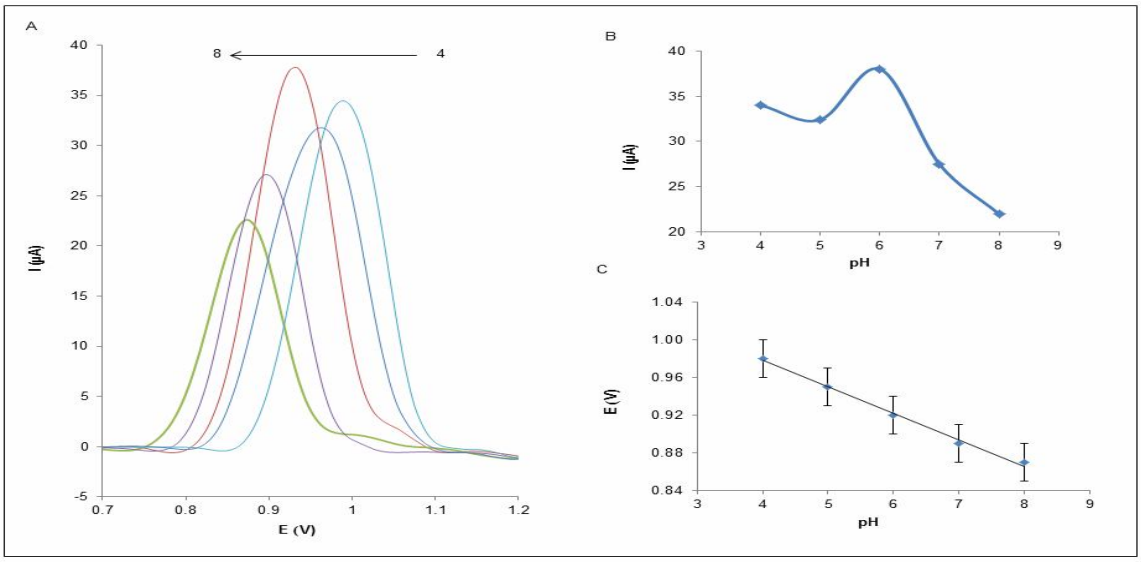

Fig. 6. A) DPV of 10 µM Tz on AuNPs/rGO/AEP/SPE in 0.1 M PBS solution; B) I as a function of pH; and C) E as function of pH.

DPV Investigations on AuNPs/rGO/AEP/SPE for Electrochemical Oxidation of Tz

Differential pulse voltammetry (DPV) is a sensitive analytical method in which the charging current is decreased. Compared to the CV technique, the resulting redox peak potential of the target analyte is more negative for DPV. Thus, Tz's electrochemical oxidation on the AuNPs/rGO/AEP/SPE modified electrode was surveyed by DPV. Figure 5A shows the DPV curve of the AuNPs/rGO/AEP/SPE by increasing Tz concentration in 0.1 M PBS (pH 6) electrolytes. This finding revealed that Tz was effectively electrochemically oxidized on the surface of AuNPs/rGO/AEP/SPE electrode. The inset reveals the corresponding linear calibration plots for different concentrations *versus* current values with R^2 = 0.9957 (Fig. 6B). The calculated linear ranges ranged from

Table 1. Comparison of the Effectiveness of Several Modified Electrodes Utilized in Tz Electrocatalysis

Sr. No.	Electrode substrate	Dyes detected	Measurement techniques	Concentration range	LOD	Ref.
1	GO/MWCNTs	Tz	DPV	0.09-8.0 µM	0.01 µM	[33]
2	AuNPs/CPE	Tz	DPV	0.05-1.5 µM	17 nM	[34]
3	Exfoliated graphite/GCE	Tz	DPV	0.009-0.112 µM	2.8 nM	[12]
4	MWNTs/IL@PtNP/GCE	Tz	DPV	0.03-5 µM	8 nM	[35]
5	Gr-TiO_2/CPE	Tz	DPV	0.02-1.18 µM	8 nM	[36]
6	rGO/AuNPs/AEP/SPE	Tz	DPV	0.004-2 µM	3 nM	This work

0.004 µM to 2 µM. A low detection limit was provided by 3 nM sensitivity. The results were compared with those previously published in the literature, as presented in Table 1. Limit detection was lower for Tz than for other modified electrodes due to carbon. Bio nanocomposite AuNPs/rGO/AEP/SPE spotting on SPE surface was used as a unique and new method of providing an active material for efficient Tz sensing.

pH Impact on Tz Oxidation Peak

In the pH range of 4.0 to 8.0 in PBS (0.1 M), the voltammetric response of AuNPs/rGO/AEP/SPE to oxidation Tz peak was recorded (Fig. 6). As pH was increased, the Tz oxidation peak current was increased, and the maximum Tz oxidation peak current was recorded at pH 6.0. Increasing the pH value to 8.0 considerably reduced the oxidation peak current of Tz. Thus, the best optimal modes to determine Tz were observed at pH 6.0. Moreover, PBS at 0.1 M (pH = 6.0) was adopted as a supporting electrolyte to identify Tz. The impact of pH on oxidation peak potential was also assessed. By increasing the solution pH from 4 to 8, the anodic peak potential changed to negative potentials, revealing that protons participate in electrode reactions.

Impact of Accumulation Time

Accumulation time is the main factor influencing the Tz oxidation current. The impact of accumulation time on Tz oxidation peak current on AuNPs/rGO/AEP/SPE in 0.1 M PBS was surveyed. Oxidation peak current was gradually increased by one min accumulation time. Thus, oxidation peak current starts to increase partly after one min

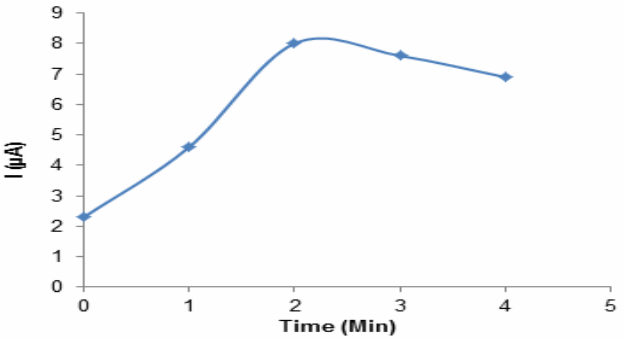

Fig. 7. The impacts of accumulation time on oxidation peak currents of 100 nM Tz.

accumulation time. Two min accumulation duration was adopted to identify Tz concentration. Then, ip_a remained stable based on the saturation adsorption of Tz on the AuNPs/rGO/AEP/SPE surface. Moreover, two min was adopted as the optimal accumulation time (Fig. 7).

Effect of Scan Rates

Using CV, the effects of scan rate on Tz oxidation peaks on the AuNPs/rGO/AEP/SPE electrode were examined. The scan rate was changed from 10 to 180 mV s^{-1} in this study, and the findings were recorded. The oxidation currents increased as the scan rate rose, as illustrated in Fig. 8A. Simultaneously, the peak oxidation potential moved slightly to the positive. The oxidation current and the scan rate have a good linear relationship, as shown in Fig. 8A. The following linear regression equations were discovered:

$$I_{pa}\ (\mu A) = 0.4111\ \nu\ (mV\ s^{-1}) + 8.7257, \qquad R^2 = 0.9904$$

They show that Tz-related electrochemical reactions in the

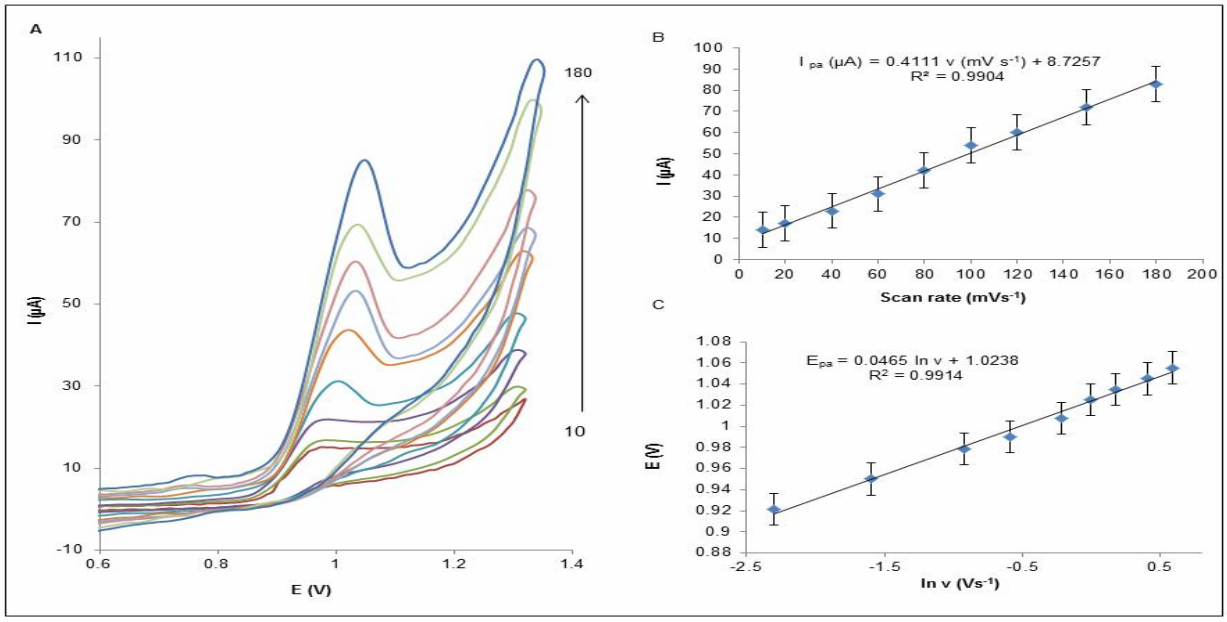

Fig. 8. (A) CVs of Tz at 10 µM on the AuNPs/rGO/AEP/SPE at various scan rates; (B) The relationship between oxidation peak current and scan rate; (C) The relationship between peak potential and the scan rate's Napierian logarithm.

AuNPs/rGO/AEP/SPE electrode are adsorption controlled [30]. Furthermore, only a positive oxidation peak potential (E_{pa}) shifts with increasing scan rates (ν), indicating that the Tz oxidation process is irreversible. Also shown is the linear relationship between E_{pa} and the Napierian logarithm of the scan rate (lnν) (Fig. 8C). The linear equation was $E_{pa} = 0.0465\ \ln\nu + 1.0238$ ($R^2 = 0.9914$). According to the Lavrion equation:

$$E_p = E^0 - \frac{2RT}{\alpha nF}\left[0.780 + \ln\left(\frac{D^{\frac{1}{2}}}{K^\circ}\right) + \ln\left(\frac{\alpha nF\nu}{RT}\right)^{\frac{1}{2}}\right]$$

$$= K^\circ + \frac{2RT}{\alpha nF}\ln\nu$$

where $E^{0'}$ is the formal potential (V), α is the charge transfer coefficient, n is the electron transfer number, F is the Faraday constant (96480 C mol^{-1}), R is the ideal gas constant (8.314 J mol^{-1} K^{-1}), T is the Kelvin temperature (K), D is the diffusion coefficient, and K° is the heterogeneous electron transfer rate. The value of α is always supposed to be 0.5 in an irreversible process, and the n value is calculated as one. Thus, the oxidation of Tz is an irreversible process with one electron and one proton. Figure 9 shows the electrochemical oxidation mechanism of Tz.

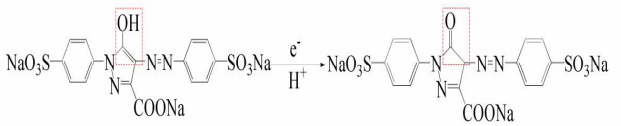

Fig. 9. The mechanism of electrochemical oxidation of Tz on AuNPs/rGO/AEP/SPE.

Reproducibility and Stability

To estimate the reproducibility of the developed method, six AuNPs/rGO/AEP/SPEs were provided and the oxidation peak current of 1.0×10^{-6} M Tz was estimated on each electrode. By comparing various electrode responses, the relative standard deviation (RSD) of tests was found to be 2.33% for Tz, indicating that the suggested approach had high reproducibility. Modified electrode repeatability was assessed by consequent recordings at a constant concentration of 1 µM Tz. Peak current RSD in DPVs for six repetitions was 1.1% Tz, proving the perfect response repeatability of the modified electrode.

AuNPs/rGO/AEP/SPE stability was investigated over a 2-week period through periodic measurement of oxidation peak currents. The results indicated that primitive response was reduced by only 4.3% Tz after the 2-week period, revealing high AuNPs/rGO/AEP/SPE stability.

Real Sample Detection

Real sample analysis was done using the DPV method to assess AuNPs/rGO/AEP/SPE modified electrode practicability. A standard addition approach was used for Tz measurement in real samples (soft drinks). The results are showed in Table 2. Samples were provided from a shop in Urmia City, Iran. Due to DPV current responses for multiple Tz concentrations, the recovery rate was computed from 98% to 101%. These results revealed that AuNPs/rGO/AEP/SPE could be utilized as an efficient system to detect Tz in soft drink samples.

Interference Studies

Interference studies were done on various interfering species and food colorants co-existing with Tz. Different sorts of interfering species were added into 0.1 M PBS (pH = 6) involving 1 µM Tz and the provided peak currents were recorded and compared. 100-times higher (contrasted with Tz concentration) concentrations of glucose, benzoic acid, citric acid, Na^+, K^+, and Fe^{3+} and 10-times higher concentrations of sunset yellow and amaranth dyes did not interfere with Tz detection. Moreover, Tz peak current intensities in the presence of interferents were the same as pure Tz, *i.e.* oxidation peaks of interfering species were isolated well from Tz. The results revealed that AuNPs/rGO/AEP/SPE had excellent anti-interference effectiveness, which gave it tremendous potential for Tz detection in multiple actual samples. Thus, it was concluded that modified electrodes were selective for detecting Tz.

Table 2. Tz Determination in Soft Drink Samples by AuNPs/rGO/APE/SPE (n = 3)

Samples	Synthetic dyes	Added (µM)	Found (µM)	Recovery (%)	RSD (%)
Soft drinks	Tz	-	-	-	-
		4	3.98	99	1.23
		6	6.06	101	1.72
		8	7.93	99.12	1.65

CONCLUSIONS

In summary, an easy and greatly effective sensor was fabricated by AuNPs, decreased graphene rGO, and acetone-extracted propolis (AEP) as a biocomposite modified screen-printed electrode for Tz detection. Modified electrodes possessed excellent structural features like prominent electrocatalytic activity, good electrical conductivity, high surface area, and high stability to the electrochemical oxidation of Tz. Wide linear range (0.004 to 2 µM) and low detection limit (3 nM) encouraged the use of grapheme, metal compositions, and acetone-extracted propolis as a biocomposite to detect electroactive biomolecules in daily life.

REFERENCES

[1] M. Sakthivel, M. Sivakumar, S.-M. Chen, K. Pandi, Sens. Actuators B Chem. 256 (2018) 195.
[2] Z.-Z. An, Z. Li, Y.-Y. Guo, X.-L. Chen, K.-N. Zhang, D.-X. Zhang, Z.-H. Xue, X.-B. Zhou, X.-Q. Lu, Chin. Chem. Lett. 28 (2017) 1492.
[3] Y.S. Al-Degs, Food Chem. 117 (2009) 485.
[4] E. Dinç, E. Baydan, M. Kanbur, F. Onur, Talanta 58 (2002) 579.
[5] J. Berzas, J.R. Flores, M.V. Llerena, N.R. Farinas, Anal. Chim. Acta 391 (1999) 353.
[6] M. Yamada, M. Nakamura, T. Yamada, T. Maitani, Y. Goda, Chem. Pharm. Bull. 44 (1996) 1624.
[7] T. Zou, P. He, A. Yasen, Z. Li, Food Chem. 138 (2013) 1742.
[8] S.M. Ghoreishi, M. Behpour, M. Golestaneh, Anal. Methods 3 (2011) 2842.
[9] C. Wu, Q. Cheng, K. Wu, G. Wu, Q. Li, Anal. Chim. Acta 825 (2014) 26.
[10] B. Rui, M. Yang, L. Zhang, Y. Jia, Y. Shi, R. Histed, Y. Liao, J. Xie, F. Lei, L. Fan, J. Appl. Electrochem. (2020) 1.
[11] Y.H. Yu, W.S. Wang, Y.C. Hu, C.H. Tsai, C.J. Shih, W.C. Huang, S.M. Peng, G.H. Lee, J. Chin. Chem.

Soc. 66 (2019) 996.
[12] X. Song, Z. Shi, X. Tan, S. Zhang, G. Liu, K. Wu, Sens. Actuators B Chem. 197 (2014) 104.
[13] S.T. Huang, Y. Shi, N.B. Li, H.Q. Luo, Analyst. 137 (2012) 2593.
[14] T. Gan, J. Sun, S. Cao, F. Gao, Y. Zhang, Y. Yang, Electrochim. Acta 74 (2012) 151.
[15] H. Han, D. Pan, X. Wu, Q. Zhang, H. Zhang, J. Mater. Sci. 49 (2014) 4796.
[16] N. Shams, H.N. Lim, R. Hajian, N.A. Yusof, J. Abdullah, Y. Sulaiman, I. Ibrahim, N.M. Huang, A. Pandikumar, J. Appl. Electrochem. 46 (2016) 655.
[17] L. Ding, Y. Liu, J. Zhai, A.M. Bond, J. Zhang, Electroanalysis 26 (2014) 121.
[18] B. Hausen, E. Wollenweber, H. Senff, B. Post, Contact Derm. 17 (1987) 163.
[19] E. Mascheroni, V. Guillard, F. Nalin, L. Mora, L. Piergiovanni, J. Food Eng. 98 (2010) 294.
[20] K.I. Wolska, A.M. Grudniak, B. Fiecek, A. Kraczkiewicz-Dowjat, A. Kurek, Cent. Eur. J. Biol. 5 (2010) 543.
[21] L.H. Yao, Y.-M. Jiang, J. Shi, F. Tomas-Barberan, N. Datta, R. Singanusong, S. Chen, Plant Foods Hum. Nutr. 59 (2004) 113.
[22] W. Krol, S. Scheller, Z. Czuba, T. Matsuno, G. Zydowicz, J. Shani, M. Mos, J. Ethnopharmacol. 55 (1996) 19.
[23] K. Shimizu, H. Ashida, Y. Matsuura, K. Kanazawa, Arch. Biochem. 424 (2004) 181.
[24] Z. Warakomska, W. Maciejewicz, Apidologie 23 (1992) 277.
[25] G. Girgin, T. Baydar, M. Ledochowski, H. Schennach, D.N. Bolukbasi, K. Sorkun, B. Salih, G. Sahin, D. Fuchs, Immunobiology 214 (2009) 129.
[26] M. Huleihel, V. Pavlov, V. Erukhimovitch, J. Photochem. Photobiol. B 96 (2009) 17.
[27] F. Kheiri, R. Sabzi, E. Jannatdoust, E. Shojaeefar, H. Sedghi, Biosens. Bioelectron. 26 (2011) 4457.
[28] W.S. Hummers Jr, R.E. Offeman, J. Am. Chem. Soc. 80 (1958) 1339.
[29] H. Chen, Z. Zhang, R. Cai, W. Rao, F. Long, Electrochim. Acta 117 (2014) 385.
[30] Q. He, J. Liu, X. Liu, G. Li, P. Deng, J. Liang, D. Chen, Sensors 18 (2018) 1911.
[31] B. Rezaei, N. Majidi, H. Rahmani, T. Khayamian, Biosens. Bioelectron. 26 (2011) 2130.
[32] J. Du, R. Yue, Z. Yao, F. Jiang, Y. Du, P. Yang, C. Wang, Colloids Surf. 419 (2013) 94.
[33] X. Qiu, L. Lu, J. Leng, Y. Yu, W. Wang, M. Jiang, L. Bai, Food Chem. 190 (2016) 889.
[34] S.M. Ghoreishi,M. Behpour, M. Golestaneh, J. Chin. Chem. Soc. 60 (2013) 120.
[35] L. Zhao, B. Zeng, F. Zhao, Electrochim. Acta 146 (2014) 611.
[36] T. Gan, J. Sun, W. Meng, L. Song, Y. Zhang, Food Chem. 141 (2013) 3731.